# Direct Solution of Renormalization Group Equations of QCD in $x-$space:
## NLO Implementations at Leading Twist

Alessandro Cafarella and Claudio Corianò

*Dipartimento di Fisica, Università di Lecce and INFN sezione di Lecce*
*Via per Arnesano, 73100 Lecce, Italy*[1]
*and*
*Department of Physics and Institute for Plasma Physics, Univ. of Crete*
*and FO.R.T.H., 71003 Heraklion, Greece*
*e-mail: alessandro.cafarella@le.infn.it, claudio.coriano@le.infn.it*



**Abstract**

We illustrate the implementation of a method based on the use of recursion relations in (Bjorken) $x-$space for the solution of the evolution equations of QCD for all the leading twist distributions. The algorithm has the advantage of being very fast. The implementation that we release is written in C and is performed to next-to-leading order in $\alpha_s$.

[1]Permanent Address

# Program summary

- *Title of program:* `evolution.c`
- *Computer:* Athlon 1800 plus
- *Operating system under which the program has been tested:* Linux
- *Programming language used:* C
- *Peripherals used:* Laser printer
- *No. of bytes in distributed program:* 20771
- *Keywords:* Polarized and unpolarized parton distribution, numerical solutions of renormalization group equation in Quantum Chromodynamics.
- *Nature of physical problem:* The program provided here solves the DGLAP evolution equations to next-to-leading order $\alpha_s$, for unpolarized, longitudinally polarized and transversely polarized parton distributions.
- *Method of solution:* We use a recursive method based on an expansion of the solution in powers of $\log\left(\alpha_s(Q)/\alpha_s(Q_0)\right)$
- *Typical running time:* About 1 minute and 30 seconds for the unpolarized and longitudinally polarized cases and 1 minute for the transversely polarized case.

# LONG WRITE UP

# 1 Introduction

Our understanding of the QCD dynamics has improved steadily along the years. In fact we can claim that precision studies of the QCD background in a variety of energy ranges, from intermediate to high energy - whenever perturbation theory and factorization theorems hold - are now possible and the level of accuracy reached in this area is due both to theoretical improvements and to the flexible numerical implementations of many of the algorithms developed at theory level.

Beside their importance in the determination of the QCD background in the search of new physics, these studies convey an understanding of the structure of the nucleon from first principles, an effort which is engaging both theoretically and experimentally.

It should be clear, however, that perturbative methods are still bound to approximations, from the order of the perturbative expansion to the phenomenological description of the parton distribution functions, being them related to a parton model view of the QCD dynamics.

Within the framework of the parton model, evolution equations of DGLAP-type - and the corresponding initial conditions on the parton distributions - are among the most important blocks which characterize the description of the quark-gluon interaction and, as such, deserve continuous attention. Other parts of this description require the computation of hard scatterings with high accuracy and an understanding of the fragmentation region as well. The huge success of the parton model justifies all the effort.

In this consolidated program, we believe that any attempt to study the renormalization group evolution describing the perturbative change of the distributions with energy, from a different - in this case, numerical - standpoint is of interest.

In this paper we illustrate an algorithm based on the use of recursion relations for the solution of evolution equations of DGLAP type. We are going to discuss some of the salient features of the method and illustrate its detailed implementation as a computer code up to next-to leading order (NLO) in $\alpha_s$, the strong coupling constant.

In this context, it is worth to recall that the most common method implemented so far in the solution of the DGLAP equations is the one based on the Mellin moments, with all its good points and limitations.

The reason for such limitations are quite obvious: while it is rather straightforward to solve the equations in the space of moments, their correct inversion is harder to perform, since this requires the computation of an integral in the complex plane and the search for an optimized path.

In this respect, several alternative implementations of the NLO evolution are available from the previous literature, either based on the use of "brute force" algorithms [1] or on the Laguerre expansion [2, 3], all with their positive features and their limitations.

Here we document an implementation to NLO of a method based on an ansatz [4] which allows to rewrite the evolution equations as a set of recursion relations for some scale invariant functions, $A_n(x)$ and $B_n(x)$, which appear in the expansion. The advantage, compared to others, of using these recursion relations is that just few iterates of these are necessary in order to obtain a stable solution. The number of iterates is determined at run time. We also mention that our implementation can be extended to more complex cases, including the cases of nonforward parton distributions and of supersymmetry, which will be discussed elsewhere . Here we have implemented the recursion method in all the important cases of initial state scaling violations connected to the evolutions of both polarized and unpolarized parton densities, including the less known transverse spin distributions.

Part of this document is supposed to illustrate the algorithm, having worked out in some detail the structure of the recursion relations rather explicitly, especially in the case of non-singlet evolutions, such as for transverse spin distributions. As we have mentioned, the same method has also been applied successfully to the case of supersymmetric QCD and will be illustrated in a companion paper.

One of the advantages of the method is its analytical base, since the recursion relations can be written down in explicit form and at the same time one can perform a simple analytical matching between various regions in the evolutions, which is a good feature of x-spaced methods. While this last aspect is not relevant for ordinary QCD, it is relevant in other theories, such as for supersymmetric extensions of the parton model, once one assumes that, as the evolution scale $Q$ raises, new anomalous dimensions are needed in order to describe the mixing between ordinary and supersymmetric partons.

## 2 Definitions and Conventions

In this section we briefly outline our definitions and conventions.

We will be using the running of the coupling constant up to two-loop level

$$\alpha_s(Q^2) = \frac{4\pi}{\beta_0}\frac{1}{\log(Q^2/\Lambda^2_{\overline{MS}})}\left[1 - \frac{\beta_1}{\beta_0^2}\frac{\log\log(Q^2/\Lambda^2_{\overline{MS}})}{\log(Q^2/\Lambda^2_{\overline{MS}})} + O\left(\frac{1}{\log^2(Q^2/\Lambda^2_{\overline{MS}})}\right)\right], \qquad (1)$$

where

$$\beta_0 = \frac{11}{3}N_C - \frac{4}{3}T_f, \qquad \beta_1 = \frac{34}{3}N_C^2 - \frac{10}{3}N_C n_f - 2C_F n_f, \qquad (2)$$

and

$$N_C = 3, \qquad C_F = \frac{N_C^2 - 1}{2N_C} = \frac{4}{3}, \qquad T_f = T_R n_f = \frac{1}{2} n_f, \tag{3}$$

where $N_C$ is the number of colors, $n_f$ is the number of active flavors, which is fixed by the number of quarks with $m_q \leq Q$. We have taken for the quark masses $m_c = 1.5\,\mathrm{GeV}, m_b = 4.5\,\mathrm{GeV}$ and $m_t = 175\,\mathrm{GeV}$, these are necessary in order to identify the thresholds at which the number of flavours $n_f$ is raised as we increase the final evolution scale.

In our conventions $\Lambda_{QCD}$ is denoted by $\Lambda_{\overline{MS}}^{(n_f)}$ and is given by

$$\Lambda_{\overline{MS}}^{(3,4,5,6)} = 0.248,\, 0.200,\, 0.131,\, 0.050\,\mathrm{GeV}. \tag{4}$$

We also define the distribution of a given helicity ($\pm$), $f^{\pm}(x, Q^2)$, which is the probability of finding a parton of type $f$ at a scale $Q$, where $f = q_i, \overline{q_i}, g$, in a longitudinally polarized proton with the spin aligned (+) or anti-aligned (-) respect to the proton spin and carrying a fraction $x$ of the proton's momentum.

As usual, we introduce the longitudinally polarized parton distribution of the proton

$$\Delta f(x, Q^2) \equiv f^+(x, Q^2) - f^-(x, Q^2). \tag{5}$$

We also introduce another type of parton density, termed *transverse spin distribution*, which is defined as the probability of finding a parton of type $f$ in a transversely polarized proton with its spin parallel ($\uparrow$) minus the probability of finding it antiparallel ($\downarrow$) to the proton spin

$$\Delta_T f(x, Q^2) \equiv f^{\uparrow}(x, Q^2) - f^{\downarrow}(x, Q^2). \tag{6}$$

Similarly, the unpolarized (spin averaged) parton distribution of the proton is given by

$$f(x, Q^2) \equiv f^+(x, Q^2) + f^-(x, Q^2) = f^{\uparrow}(x, Q^2) + f^{\downarrow}(x, Q^2). \tag{7}$$

We also recall, if not obvious, that taking linear combinations of Equations (7) and (5), one recovers the parton distributions of a given helicity

$$f^{\pm}(x, Q^2) = \frac{f(x, Q^2) \pm \Delta f(x, Q^2)}{2}. \tag{8}$$

In regard to the kernels, the notations $P$, $\Delta P$, $\Delta_T P$, $P^{+\pm}$, will be used to denote the Altarelli-Parisi kernels in the unpolarized, longitudinally polarized, transversely polarized, and the positive (negative) helicity cases respectively.

Let us now turn to the evolution equations, starting from the unpolarized case. Defining

$$q_i^{(\pm)} = q_i \pm \overline{q_i}, \qquad q^{(+)} = \sum_{i=1}^{n_f} q_i^{(+)}, \qquad \chi_i = q_i^{(+)} - \frac{1}{n_f} q^{(+)}, \tag{9}$$

and introducing the convolution product

$$f(x) \otimes g(x) = \int_x^1 \frac{\mathrm{d}y}{y} f\left(\frac{x}{y}\right) g(y), \tag{10}$$

the evolution equations are

$$\frac{\mathrm{d}}{\mathrm{d}\log Q^2} q_i^{(-)}(x, Q^2) = P_{NS^-}(x, \alpha_s(Q^2)) \otimes q_i^{(-)}(x, Q^2), \tag{11}$$

$$\frac{\mathrm{d}}{\mathrm{d}\log Q^2} \chi_i(x, Q^2) = P_{NS^+}(x, \alpha_s(Q^2)) \otimes \chi_i(x, Q^2), \tag{12}$$

for the non-singlet sector and

$$\frac{\mathrm{d}}{\mathrm{d}\log Q^2}\begin{pmatrix} q^{(+)}(x,Q^2) \\ g(x,Q^2)\end{pmatrix} = \begin{pmatrix} P_{qq}(x,\alpha_s(Q^2)) & P_{qg}(x,\alpha_s(Q^2)) \\ P_{gq}(x,\alpha_s(Q^2)) & P_{gg}(x,\alpha_s(Q^2))\end{pmatrix} \otimes \begin{pmatrix} q^{(+)}(x,Q^2) \\ g(x,Q^2)\end{pmatrix} \quad (13)$$

for the singlet sector. Equations analogous to (9-13), with just a change of notation, are valid in the longitudinally polarized case and, due to the linearity of the evolution equations, also for the distributions in the helicity basis. In the transverse case instead, there is no coupling between gluons and quarks, so the singlet sector (13) is missing. In this case we will solve just the nonsinglet equations

$$\frac{\mathrm{d}}{\mathrm{d}\log Q^2}\Delta_T q_i^{(-)}(x,Q^2) = \Delta_T P_{NS^-}(x,\alpha_s(Q^2)) \otimes \Delta_T q_i^{(-)}(x,Q^2), \quad (14)$$

$$\frac{\mathrm{d}}{\mathrm{d}\log Q^2}\Delta_T q_i^{(+)}(x,Q^2) = \Delta_T P_{NS^+}(x,\alpha_s(Q^2)) \otimes \Delta_T q_i^{(+)}(x,Q^2). \quad (15)$$

We also recall that the perturbative expansion, up to next-to-leading order, of the kernels is

$$P(x,\alpha_s) = \left(\frac{\alpha_s}{2\pi}\right) P^{(0)}(x) + \left(\frac{\alpha_s}{2\pi}\right)^2 P^{(1)}(x) + \ldots. \quad (16)$$

Kernels of fixed helicity can also be introduced with $P_{++}(z) = (P(z) + \Delta P(z))/2$ and $P_{+-}(z) = (P(z) - \Delta P(z))/2$ denoting splitting functions of fixed helicity, which will be used below.

The equations, in the helicity basis, are

$$\begin{aligned}
\frac{dq_+(x)}{dt} &= \frac{\alpha_s}{2\pi}(P^{qq}_{++}(\frac{x}{y}) \otimes q_+(y) + P^{qq}_{+-}(\frac{x}{y}) \otimes q_-(y) \\
&\quad + P^{qg}_{++}(\frac{x}{y}) \otimes g_+(y) + P^{qg}_{+-}(\frac{x}{y}) \otimes g_-(y)), \\
\frac{dq_-(x)}{dt} &= \frac{\alpha_s}{2\pi}(P_{+-}(\frac{x}{y}) \otimes q_+(y) + P_{++}(\frac{x}{y}) \otimes q_-(y) \\
&\quad + P^{qg}_{+-}(\frac{x}{y}) \otimes g_+(y) + P^{qg}_{++}(\frac{x}{y}) \otimes g_-(y)), \\
\frac{dg_+(x)}{dt} &= \frac{\alpha_s}{2\pi}(P^{gq}_{++}(\frac{x}{y}) \otimes q_+(y) + P^{gq}_{+-}(\frac{x}{y}) \otimes q_-(y) \\
&\quad + P^{gg}_{++}(\frac{x}{y}) \otimes g_+(y) + P^{gg}_{+-}(\frac{x}{y}) \otimes g_-(y)), \\
\frac{dg_-(x)}{dt} &= \frac{\alpha_s}{2\pi}(P^{gq}_{+-}(\frac{x}{y}) \otimes q_+(y) + P^{gq}_{++}(\frac{x}{y}) \otimes q_-(y) \\
&\quad + P^{g}_{+-}(\frac{x}{y}) \otimes g_+(y) + P^{gg}_{++}(\frac{x}{y}) \otimes g_-(y)).
\end{aligned} \quad (17)$$

The non-singlet (valence) analogue of this equation is also easy to write down

$$\begin{aligned}
\frac{dq_{+,V}(x)}{dt} &= \frac{\alpha_s}{2\pi}(P_{++}(\frac{x}{y}) \otimes q_{+,V}(y) + P_{+-}(\frac{x}{y}) \otimes q_{-,V}(y)), \\
\frac{dq_{-,V}(x)}{dt} &= \frac{\alpha_s}{2\pi}(P_{+-}(\frac{x}{y}) \otimes q_{+,V}(y) + P_{++}(\frac{x}{y}) \otimes q_{-,V}(y)).
\end{aligned} \quad (18)$$

where the $q_{\pm,V} = q_\pm - \bar{q}_\pm$ are the valence components of fixed helicity. The kernels in this basis are given by

$$P^{(0)}_{NS\pm,++} = P^{(0)}_{qq,++} = P^{(0)}_{qq}$$

$$
\begin{aligned}
P^{(0)}_{qq,+-} &= P^{(0)}_{qq,-+} = 0 \\
P^{(0)}_{qg,++} &= n_f x^2 \\
P_{qg,+-} &= P_{qg,-+} = n_f (x-1)^2 \\
P_{gq,++} &= P_{gq,--} = C_F \frac{1}{x} \\
P^{(0)}_{gg,++} &= P^{(0)}_{gg,++} = N_c \left( \frac{2}{(1-x)_+} + \frac{1}{x} - 1 - x - x^2 \right) + \beta_0 \delta(1-x) \\
P^{(0)}_{gg,+-} &= N_c \left( 3x + \frac{1}{x} - 3 - x^2 \right).
\end{aligned} \tag{19}
$$

Taking linear combinations of these equations (adding and subtracting), one recovers the usual evolutions for unpolarized $q(x)$ and longitudinally polarized $\Delta q(x)$ distributions.

# 3 The Ansatz and some Examples

In order to solve the evolution equations directly in $x$-space, we assume solutions of the form

$$
f(x,Q^2) = \sum_{n=0}^{\infty} \frac{A_n(x)}{n!} \log^n \frac{\alpha_s(Q^2)}{\alpha_s(Q_0^2)} + \alpha_s(Q^2) \sum_{n=0}^{\infty} \frac{B_n(x)}{n!} \log^n \frac{\alpha_s(Q^2)}{\alpha_s(Q_0^2)}, \tag{20}
$$

for each parton distribution $f$, where $Q_0$ defines the initial evolution scale. The justification of this ansatz can be found, at least in the case of the photon structure function, in the original work of Rossi [4], and its connection to the ordinary solutions of the DGLAP equations is most easily worked out by taking moments of the scale invariant coefficient functions $A_n$ and $B_n$ and comparing them to the corresponding moments of the parton distributions, as we are going to illustrate in section 5. The link between Rossi's expansion and the solution of the evolution equations (which are ordinary differential equations) in the space of the moments up to NLO will be discussed in that section, from which it will be clear that Rossi's ansatz involves a resummation of the ordinary Mellin moments of the parton distributions.

Setting $Q = Q_0$ in (20) we get

$$
f(x,Q_0^2) = A_0(x) + \alpha_s(Q_0^2) B_0(x). \tag{21}
$$

Inserting (20) in the evolution equations, we obtain the following recursion relations for the coefficients $A_n$ and $B_n$

$$
A_{n+1}(x) = -\frac{2}{\beta_0} P^{(0)}(x) \otimes A_n(x), \tag{22}
$$

$$
B_{n+1}(x) = -B_n(x) - \frac{\beta_1}{4\beta_0} A_{n+1}(x) - \frac{2}{\beta_0} P^{(0)}(x) \otimes B_n(x) - \frac{1}{4\pi\beta_0} P^{(1)}(x) \otimes A_n(x), \tag{23}
$$

obtained by equating left-hand sides and right-hand-side of the equation of the same logarithmic power in $\log^n \alpha_s(Q^2)$ and $\alpha_s \log^n \alpha_s(Q^2)$.

Any boundary condition satisfying (21) can be chosen at the lowest scale $Q_0$ and in our case we choose

$$
B_0(x) = 0, \qquad f(x,Q_0^2) = A_0(x). \tag{24}
$$

The actual implementation of the recursion relations is the main effort in the actual writing of the code. Obviously, this requires particular care in the handling of the singularities in $x-$space, being all the kernels defined as distributions. Since the distributions

are integrated, there are various ways to render the integrals finite, as discussed in the previous literature on the method [5] in the case of the photon structure function. In these previous studies the edge-point contributions - i.e. the terms which multiply $\delta(1-x)$ in the kernels - are approximated using a sequence of functions converging to the $\delta$ function in a distributional sense.

This technique is not very efficient. We think that the best way to proceed is to actually perform the integrals explicitly in the recursion relations and let the subtracting terms appear under the same integral together with the bulk contributions ($x < 1$) (see also [6]). This procedure is best exemplified by the integral relation

$$\int_x^1 \frac{dy}{y(1-y)_+} f(x/y) = \int_x^1 \frac{dy}{y} \frac{yf(y) - xf(x)}{y-x} - \log(1-x) f(x) \tag{25}$$

in which, on the right hand side, regularity of both the first and the second term is explicit. For instance, the evolution equations become (prior to separation between singlet and non-singlet sectors) in the unpolarized case

$$\begin{aligned}
\frac{dq_i(x)}{d\log(Q^2)} &= 2C_F \int \frac{dy}{y} \frac{yq_i(y) - xq_i(x)}{y-x} + 2C_F \log(1-x) q_i(x) - \int_x^1 \frac{dy}{y} (1+z)\, q_i(y) + \frac{3}{2} C_F q(x) \\
&\quad + n_f \int_x^1 \frac{dy}{y} \left( z^2 + (1-z)^2 \right) g(y) \\
\frac{dg(x)}{d\log(Q^2)} &= C_F \int_x^1 \frac{dy}{y} \frac{1+(1-z)^2}{z} q_i(y) + 2N_c \int_x^1 \frac{dy}{y} \frac{yf(y) - xf(x)}{y-x} g(y) \\
&\quad + 2N_c \log(1-x) g(x) + 2N_c \int_x^1 \frac{dy}{y} \left( \frac{1}{z} - 2 + z(1-z) \right) g(y) + \frac{\beta_0}{2} g(x)
\end{aligned} \tag{26}$$

with $z \equiv x/y$. Here $q$ are fixed flavour distributions.

# 4 An Example: The Evolution of the Transverse Spin Distributions

Leading order (LO) and NLO recursion relations for the coefficients of the expansion can be worked out quite easily. We illustrate here in detail the implementation of a non-singlet evolutions, such as those involving transverse spin distributions. For the first recursion relation (22) in this case we have

$$\begin{aligned}
&A_{n+1}^{\pm}(x) = -\frac{2}{\beta_0} \Delta_T P_{qq}^{(0)}(x) \otimes A_n^{\pm}(x) = \\
&C_F \left( -\frac{4}{\beta_0} \right) \left[ \int_x^1 \frac{dy}{y} \frac{yA_n^{\pm}(y) - xA_n^{\pm}(x)}{y-x} + A_n^{\pm}(x) \log(1-x) \right] + \\
&C_F \left( \frac{4}{\beta_0} \right) \left( \int_x^1 \frac{dy}{y} A_n^{\pm}(y) \right) + C_F \left( -\frac{2}{\beta_0} \right) \frac{3}{2} A_n^{\pm}(x)\,.
\end{aligned} \tag{27}$$

As we move to NLO, it is convenient to summarize the structure of the transverse kernel $\Delta_T P_{qq}^{\pm,(1)}(x)$ as

$$\begin{aligned}
&\Delta_T P_{qq}^{\pm,(1)}(x) = K_1^{\pm}(x)\delta(1-x) + K_2^{\pm}(x) S_2(x) + K_3^{\pm}(x) \log(x) \\
&+ K_4^{\pm}(x) \log^2(x) + K_5^{\pm}(x) \log(x) \log(1-x) + K_6^{\pm}(x) \frac{1}{(1-x)_+} + K_7^{\pm}(x)\,.
\end{aligned} \tag{28}$$

Hence, for the (+) case we have

$$\Delta_T P_{qq}^{+,(1)}(x) \otimes A_n^+(x) = K_1^+ A_n^+(x) + \int_x^1 \frac{dy}{y} \left[ K_2^+(z) S_2(z) + K_3^+(z) \log(z) \right.$$
$$\left. + \log^2(z) K_4^+(z) + \log(z) \log(1-z) K_5^+(z) \right] A_n^+(y) +$$
$$K_6^+ \left\{ \int_x^1 \frac{dy}{y} \frac{y A_n^+(y) - x A_n^+(x)}{y-x} + A_n^+(x) \log(1-x) \right\} + K_7^+ \int_x^1 \frac{dy}{y} A_n^+(y) \,, \qquad (29)$$

where $z = x/y$. For the $(-)$ case we get a similar expression.
For the $B_{n+1}^{\pm}(x)$ we get (for the $(+)$ case)

$$B_{n+1}^+(x) = -B_n^+(x) + \frac{\beta_1}{2\beta_0^2} \left\{ 2C_F \left[ \int_x^1 \frac{dy}{y} \frac{y A_n^+(y) - x A_n^+(x)}{y-x} + A_n^+(x) \log(1-x) \right] + \right.$$
$$\left. -2C_F \left( \int_x^1 \frac{dy}{y} A_n^+(y) \right) + C_F \frac{3}{2} A_n^+(x) \right\} - \frac{1}{4\pi\beta_0} K_1^+ A_n^+(x) + \int_x^1 \frac{dy}{y} \left[ K_2^+(z) S_2(z) + \right.$$
$$\left. + K_3^+(z) \log(z) + \log^2(z) K_4^+(z) + \log(z) \log(1-z) K_5^+(z) \right] \left( -\frac{1}{4\pi\beta_0} \right) A_n^+(y) +$$
$$K_6^+ \left( -\frac{1}{4\pi\beta_0} \right) \left\{ \left[ \int_x^1 \frac{dy}{y} \frac{y A_n^+(y) - x A_n^+(x)}{y-x} + A_n^+(x) \log(1-x) \right] + K_7^+ \int_x^1 \frac{dy}{y} A_n^+(y) \right\} -$$
$$C_F \left( -\frac{4}{\beta_0} \right) \left[ \int_x^1 \frac{dy}{y} \frac{y B_n^{\pm}(y) - x B_n^{\pm}(x)}{y-x} + B_n^{\pm}(x) \log(1-x) \right] +$$
$$C_F \left( \frac{4}{\beta_0} \right) \left( \int_x^1 \frac{dy}{y} B_n^{\pm}(y) \right) + C_F \left( -\frac{2}{\beta_0} \right) \frac{3}{2} B_n^{\pm}(x)$$

where in the $(+)$ case we have the expressions

$$K_1^+(x) = \frac{1}{72} C_F(-2n_f(3+4\pi^2) + N_C(51 + 44\pi^2 - 216\zeta(3)) + 9C_F(3 - 4\pi^2 + 48\zeta(3))$$
$$K_2^+(x) = \frac{2C_F(-2C_F + N_C)x}{1+x}$$
$$K_3^+(x) = \frac{C_F(9C_F - 11N_C + 2n_f)x}{3(x-1)}$$
$$K_4^+(x) = \frac{C_F N_C x}{1-x}$$
$$K_5^+(x) = \frac{4C_F^2 x}{1-x}$$
$$K_6^+(x) = -\frac{1}{9} C_F(10n_f + N_C(-67 + 3\pi^2))$$
$$K_7^+(x) = \frac{1}{9} C_F(10n_f + N_C(-67 + 3\pi^2)), \qquad (30)$$

and for the $(-)$ case

$$K_1^-(x) = \frac{1}{72} C_F(-2n_f(3+4\pi^2) + N_C(51 + 44\pi^2 - 216\zeta(3)) + 9C_F(3 - 4\pi^2 + 48\zeta(3))$$
$$K_2^-(x) = \frac{2C_F(+2C_F - N_C)x}{1+x}$$

$$
\begin{aligned}
K_3^-(x) &= \frac{C_F(9C_F - 11N_C + 2n_f)x}{3(x-1)} \\
K_4^-(x) &= \frac{C_F N_C x}{1-x} \\
K_5^-(x) &= \frac{4C_F^2 x}{1-x} \\
K_6^-(x) &= -\frac{1}{9}C_F(10n_f + N_C(-67 + 3\pi^2)) \\
K_7^-(x) &= -\frac{1}{9}C_F(10n_f - 18C_F(x-1) + N_C(-76 + 3\pi^2 + 9x)).
\end{aligned}
\tag{31}
$$

The terms containing similar distribution (such as "+" distributions and $\delta$ functions) have been combined together in order to speed-up the computation of the recursion relations.

# 5 Comparisons among Moments

It is particularly instructing to illustrate here briefly the relation between the Mellin moments of the parton distributions, which evolve with standard ordinary differential equations, and those of the arbitrary coefficient $A_n(x)$ and $B_n(x)$ which characterize Rossi's expansion up to next-to leading order (NLO). This relation, as we are going to show, involves a resummation of the ordinary moments of the parton distributions.

Specifically, here we will be dealing with the relation between the Mellin moments of the coefficients appearing in the expansion

$$
\begin{aligned}
A(N) &= \int_0^1 dx\, x^{N-1} A(x) \\
B(N) &= \int_0^1 dx\, x^{N-1} B(x)
\end{aligned}
\tag{32}
$$

and those of the distributions

$$
\Delta_T q^{(\pm)}(N, Q^2) = \int_0^1 dx\, x^{N-1} \Delta_T q^{(\pm)}(x, Q^2)). \tag{33}
$$

For this purpose we recall that the general (non-singlet) solution to NLO for the latter moments is given by

$$
\Delta_T q_\pm(N, Q^2) = K(Q_0^2, Q^2, N) \left(\frac{\alpha_s(Q^2)}{\alpha_s(Q_0^2)}\right)^{-2\Delta_T P_{qq}^{(0)}(N)/\beta_0} \Delta_T q_\pm(N, Q_0^2)
$$

with the input distributions $\Delta_T q_\pm^n(Q_0^2)$ at the input scale $Q_0$. We also have set

$$
K(Q_0^2, Q^2, N) = 1 + \frac{\alpha_s(Q_0^2) - \alpha_s(Q^2)}{\pi\beta_0}\left[\Delta_T P_{qq,\pm}^{(1)}(N) - \frac{\beta_1}{2\beta_0}\Delta_T P_{qq\pm}^{(0)}(N)\right]. \tag{34}
$$

In the expressions above we have introduced the corresponding moments for the LO and NLO kernels ($\Delta_T P_{qq}^{(0),N}$, $\Delta_T P_{qq,\pm}^{(1),N}$).

The relation between the moments of the coefficients of the non-singlet $x-$space expansion and those of the parton distributions at any $Q$, as expressed by eq. (34) can be easily written down

$$
A_n(N) + \alpha_s B_n(N) = \Delta_T q_\pm(N, Q_0^2) K(Q_0, Q, N) \left(\frac{-2\Delta_T P_{qq}(N)}{\beta_0}\right)^n. \tag{35}
$$

As a check of this expression, notice that the initial condition is easily obtained from (35) setting $Q \to Q_0, n \to 0$, thereby obtaining

$$A_0^{NS}(N) + \alpha_s B_0^{NS}(N) = \Delta_T q_\pm(N, Q_0^2), \tag{36}$$

which can be solved with $A_0^{NS}(N) = \Delta_T q_\pm(N, Q_0^2)$ and $B_0^{NS}(N) = 0$.

It is then evident that the expansion (20) involves a resummation of the logarithmic contributions, as shown in eq. (35).

In the singlet sector we can work out a similar relation both to LO

$$A_n(N) = e_1 \left(\frac{-2\lambda_1}{\beta_0}\right)^n + e_2 \left(\frac{-2\lambda_2}{\beta_0}\right)^n \tag{37}$$

with

$$\begin{aligned}
e_1 &= \frac{1}{\lambda_1 - \lambda_2}\left(P^{(0)}(N) - \lambda_2 \mathbf{1}\right) \\
e_2 &= \frac{1}{\lambda_2 - \lambda_1}\left(-P^{(0)}(N) + \lambda_1 \mathbf{1}\right) \\
\lambda_{1,2} &= \frac{1}{2}\left(P_{qq}^{(0)}(N) + P_{gg}^{(0)}(N) \pm \sqrt{\left(P_{qq}^{(0)}(N) - P_{gg}^{(0)}(N)\right)^2 + 4P_{qg}^{(0)}(N)P_{gq}^{(0)}(N)}\right),
\end{aligned} \tag{38}$$

and to NLO

$$A_n(N) + \alpha_s B_n(N) = \chi_1 \left(\frac{-2\lambda_1}{\beta_0}\right)^n + \chi_2 \left(\frac{-2\lambda_2}{\beta_0}\right)^n, \tag{39}$$

where

$$\begin{aligned}
\chi_1 &= e_1 + \frac{\alpha}{2\pi}\left(\frac{-2}{\beta_0} e_1 \mathbf{R} e_1 + \frac{e_2 \mathbf{R} e_1}{\lambda_1 - \lambda_2 - \beta_0/2}\right) \\
\chi_2 &= e_2 + \frac{\alpha}{2\pi}\left(\frac{-2}{\beta_0} e_2 \mathbf{R} e_2 + \frac{e_1 \mathbf{R} e_2}{\lambda_2 - \lambda_1 - \beta_0/2}\right)
\end{aligned} \tag{40}$$

with

$$\mathbf{R} = P^{(1)}(N) - \frac{\beta_1}{2\beta_0} P^{(0)}(N). \tag{41}$$

We remark, if not obvious, that $A_n(N)$ and $B_n(N)$, $P^{(0)}(N)$, $P^{(1)}(N)$, in this case, are all 2-by-2 singlet matrices.

# 6 Initial conditions

As input distributions in the unpolarized case, we have used the models of Ref.[7], valid to NLO in the $\overline{\rm MS}$ scheme at a scale $Q_0^2 = 0.40\,{\rm GeV}^2$

$$\begin{aligned}
x(u-\overline{u})(x,Q_0^2) &= 0.632 x^{0.43}(1-x)^{3.09}(1+18.2x) \\
x(d-\overline{d})(x,Q_0^2) &= 0.624(1-x)^{1.0} x(u-\overline{u})(x,Q_0^2) \\
x(\overline{d}-\overline{u})(x,Q_0^2) &= 0.20 x^{0.43}(1-x)^{12.4}(1-13.3\sqrt{x}+60.0x) \\
x(\overline{u}+\overline{d})(x,Q_0^2) &= 1.24 x^{0.20}(1-x)^{8.5}(1-2.3\sqrt{x}+5.7x) \\
xg(x,Q_0^2) &= 20.80 x^{1.6}(1-x)^{4.1}
\end{aligned} \tag{42}$$

and $xq_i(x,Q_0^2) = x\overline{q_i}(x,Q_0^2) = 0$ for $q_i = s, c, b, t$.

Following [8], we have related the unpolarized input distribution to the longitudinally polarized ones

$$\begin{aligned} x\Delta u(x,Q_0^2) &= 1.019x^{0.52}(1-x)^{0.12}xu(x,Q_0^2) \\ x\Delta d(x,Q_0^2) &= -0.669x^{0.43}xd(x,Q_0^2) \\ x\Delta \overline{u}(x,Q_0^2) &= -0.272x^{0.38}x\overline{u}(x,Q_0^2) \\ x\Delta \overline{d}(x,Q_0^2) &= x\Delta\overline{u}(x,Q_0^2) \\ x\Delta g(x,Q_0^2) &= 1.419x^{1.43}(1-x)^{0.15}xg(x,Q_0^2) \end{aligned} \tag{43}$$

and $x\Delta q_i(x,Q_0^2) = x\Delta\overline{q_i}(x,Q_0^2) = 0$ for $q_i = s,c,b,t$. Being the transversity distribution experimentally unknown, following [9], we assume the saturation of Soffer's inequality

$$x\Delta_T q_i(x,Q_0^2) = \frac{xq_i(x,Q_0^2) + x\Delta q_i(x,Q_0^2)}{2}. \tag{44}$$

# 7 Names of the input parameters, variables and of the output files

## 7.1 Notations

| | | |
|---|---|---|
| 0 | gluons, $g$ | `g` |
| 1-6 | quarks, $q_i$, sorted by their mass values$(u,d,s,c,b,t)$ | `u,d,s,c,b,t` |
| 7-12 | antiquarks, $\overline{q_i}$ | `au,ad,as,ac,ab,at` |
| 13-18 | $q_i^{(-)}$ | `um,dm,sm,cm,bm,tm` |
| 19-24 | $\chi_i$ (unpolarized and longitudinally polarized cases) | `Cu,Cd,Cs,Cc,Cb,Ct` |
| | $q_i^{(+)}$ (transversely polarized case) | `Cu,Cd,Cs,Cc,Cb,Ct` |
| 25 | $q^{(+)}$ | `qp` |

## 7.2 Input parameters and variables

| | | |
|---|---|---|
| `process` | 0 | unpolarized |
| | 1 | longitudinally polarized |
| | 2 | transversely polarized |
| `spacing` | 1 | linear |
| | 2 | logarithmic |
| `GRID_PTS` | | Number of points in the grid |
| `NGP` | | Number of Gaussian points, $n_G$ |
| `ITERATIONS` | | Number of terms in the sum (20) |
| `extension` | | Extension of the output files |

| | |
|---|---|
| `step` | grid step (linear spacing case) |
| `lstep` | step in $\log_{10} x$ (logarithmic spacing case) |
| `X[i]` | $i$-th grid point, $x_i$ |
| `XG[i][j]` | $j$-th Gaussian abscissa in the range $[x_i, 1]$, $X_{ij}$ |
| `WG[i][j]` | $j$-th Gaussian weights in the range $[x_i, 1]$, $W_{ij}$ |
| `nf, Nf` | number of active flavors, $n_f$ |
| `n_evol` | progressive number of the evolution step is $n_f - 3$ |
| `Q[i]` | values of $Q$ in the corresponding grid |
| `lambda[i]` | $\Lambda^{(n_f)}_{\overline{MS}}$, where $i = n_f - 3$ |
| `A[i][j][k]` | coefficient $A_j(x_k)$ for the distribution with index $i$ |
| `B[i][j][k]` | coefficient $B_j(x_k)$ for the distribution with index $i$ |
| `beta0` | $\beta_0$ |
| `beta1` | $\beta_1$ |
| `alpha1` | $\alpha_s(Q_{in})$, where $Q_{in}$ is the lower $Q$ of the evolution step |
| `alpha2` | $\alpha_s(Q_{fin})$, where $Q_{fin}$ is the higher $Q$ of the evolution step |

### 7.3 Output files

The generic name of an output file is: `X`*`n`*`i.ext`, where

`X` is U in the unpolarized case, L in the longitudinally polarized case and T in the transversely polarized case;

*`n`* is a progressive number that indicates the scale $Q^2$ at a given stage: $n = 0$ refers to the initial scale, the highest value of $n$ refers to the final scale and the intermediate values refer to the quarks production thresholds (1 for charm, 2 for bottom and 3 for top);

`i` is the identifier of the distribution, reported in the third column of the table in subsection 7.1;

`ext` is an extension chosen by the user.

## 8 Description of the program

### 8.1 Main program

At run time, the program asks the user to select a linear or a logarithmic spacing for the $x$-axis. The logarithmic spacing is useful in order to analyze the small-$x$ behavior. Then the program stores as external variables the grid points $x_i$ and, for each of them, calls the function `gauleg` which computes the Gaussian points $X_{ij}$ and weights $W_{ij}$ corresponding to the integration range $[x_i, 1]$, with $0 \leq j \leq n_G - 1$. After that, the user is asked to enter the type of process, the final value of $Q$ and an extension for the names of the output files. At this point the program computes the initial values of the parton distributions for gluons, up, down, anti-up and anti-down (see Section 6) at the grid points and stores them in the arrays `A[i][0][k]` (see (24)), setting to zero the initial distributions of the heavier quarks.

The evolution is done in the various regions of the evolutions, all characterized by a specific flavour number. Each new flavour comes into play only when the scale $Q$ reaches the corresponding quark mass. In that case $n_f$ is increased by 1 everywhere in the program. The recurrence relations (22) and (23) are then solved iteratively for both

the nonsinglet and the singlet sector, and at the end of each energy step the evolved distributions are reconstructed via the relation (20). The distributions computed in this way become the initial conditions for the subsequent step. The numerical values of the distributions at the end of each energy step are printed to files.

## 8.2 Function `writefile`

```
void writefile(double *A,char *filename);
```

This function creates a file, whose name is contained in the string `*filename`, with an output characterized by two columns of data: the left column contains all the values of the grid points $x_i$ and the right one the corresponding values of the array `A[i]`.

## 8.3 Function `alpha_s`

```
double alpha_s(double Q,double beta0,double beta1,double lambda);
```

Given the energy scale `Q`, the first two terms of the perturbative expansion of the $\beta$-function `beta0` and `beta1` and the value `lambda` of $\Lambda_{\overline{MS}}^{(n_f)}$, `alpha_s` returns the two-loop running of the coupling constant, using the formula (1).

## 8.4 Function `gauleg`

```
void gauleg(double x1,double x2,double x[],double w[],int n);
```

This function is taken from [10] with just some minor changes. Given the lower and upper limits of integration `x1` and `x2`, and given `n`, `gauleg` returns arrays `x[0,...,n-1]` and `w[0,...,n-1]` of length `n`, containing the abscissas and weights of the Gauss-Legendre `n`-point quadrature formula.

## 8.5 Function `interp`

```
double interp(double *A,double x);
```

Given an array `A`, representing a function known only at the grid points, and a number `x` in the interval $[0,1]$, `interp` returns the linear interpolation of the function at the point `x`.

## 8.6 Function `IntGL`

```
double IntGL(int i,double kernel(double z),double *A);
```

Given an integer `i` (corresponding to a grid point $x_i$), a one variable function `kernel(z)` and an array `A`, representing a function $g(x)$ known at the grid points, `IntGL` returns the result of the integral

$$\int_{x_i}^{1} \frac{\mathrm{d}y}{y} kernel\left(\frac{x_i}{y}\right) g(x_i), \tag{45}$$

computed by the Gauss-Legendre technique.

## 8.7 Function `IntPD`

```
double IntGL(int i,double *A);
```

Given an integer `i`, to which it corresponds a grid point $x_i$, and an array `A`, representing a function $f(x)$ known at the grid points, `IntGL` returns the result of the convolution

$$\frac{1}{(1-x_i)_+} \otimes f(x_i) = \int_{x_i}^1 \frac{\mathrm{d}y}{y} \frac{y f(y) - x_i f(x_i)}{y - x_i} + f(x_i) \log(1 - x_i), \tag{46}$$

computed by the Gauss-Legendre technique.

## 8.8 Function `S2`

```
double S2(double z);
```

This function evaluates the Spence function $S_2(z)$ using the expansion

$$S_2(z) = \log z \log(1-z) - \frac{1}{4} (\log z)^2 + \frac{\pi^2}{12} + \sum_{n=1}^{\infty} \frac{(-z)^n}{n^2} \tag{47}$$

arrested at the 50th order.

## 8.9 Function `fact`

```
double fact(int n);
```

This function returns the factorial $n!$

## 8.10 Initial distributions

```
double xuv(double x);
double xdv(double x);
double xdbmub(double x);
double xubpdb(double x);
double xg(double x);
double xu(double x);
double xubar(double x);
double xd(double x);
double xdbar(double x);
double xDg(double x);
double xDu(double x);
double xDubar(double x);
double xDd(double x);
double xDdbar(double x);
```

Given the Bjorken variable `x`, these functions return the initial distributions at the input scale (see Section 6).

## 8.11 Regular part of the kernels

```
double P0NS(double z);
double P0qq(double z);
double P0qg(double z);
double P0gq(double z);
double P0gg(double z);
double P1NSm(double z);
double P1NSp(double z);
double P1qq(double z);
```

```
double P1qg(double z);
double P1gq(double z);
double P1gg(double z);
double DP0NS(double z);
double DP0qq(double z);
double DP0qg(double z);
double DP0gq(double z);
double DP0gg(double z);
double DP1NSm(double z);
double DP1NSp(double z);
double DP1qq(double z);
double DP1qg(double z);
double DP1gq(double z);
double DP1gg(double z);
double tP0(double z);
double tP1m(double z);
double tP1p(double z);
```

Given the Bjorken variable `z`, these functions return the part of the Altarelli-Parisi kernels that does not contain singularities.

# 9 Running the code

In the plots shown in this paper we have divided the interval $[0, 1]$ of the Bjorken variable $x$ in 500 subintervals (`GRID_PTS`=501), 30 Gaussian points (`NGP`=1), and we have retained 10 terms in the sum (20) (`ITERATIONS`=10). In the figures 7 and 12 the flag `spacing` has been set to 2, in order to have a logarithmically spaced grid. This feature turns useful if one intends to analyze the small-$x$ behavior. We have tested our implementation in a detailed study of Soffer's inequality up to NLO [13].

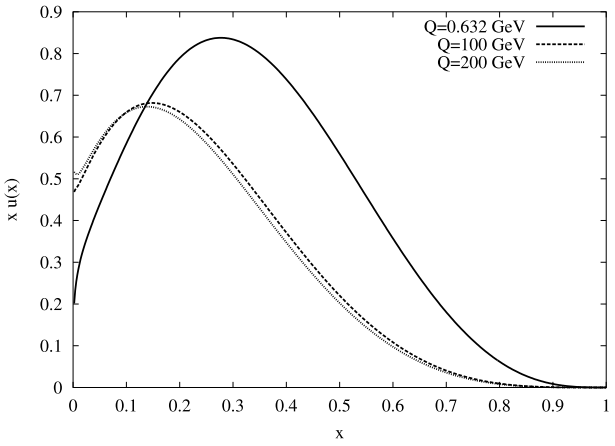


Figure 1: Evolution of the unpolarized quark up distribution $xu$ versus $x$ at various $Q$ values.

# 10 Conclusions

We have illustrated and documented a method for solving in a rather fast way the NLO evolution equations for the parton distributions at leading twist. The advantages of the method compared to other implementations based on the inversion of the Mellin moments,

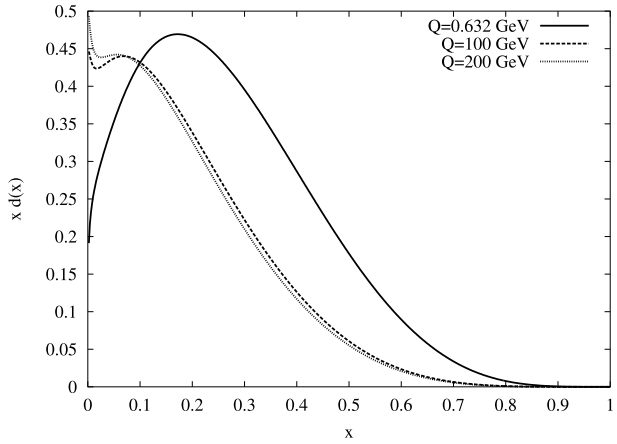


Figure 2: Evolution of $xd$ versus $x$ at various $Q$ values.

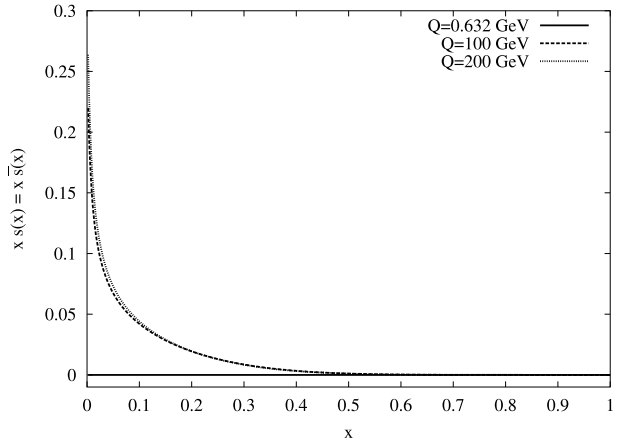


Figure 3: Evolution of $xs = x\overline{s}$ versus $x$ at various $Q$ values.

as usually done in the case of QCD, are rather evident. We have also shown how Rossi's ansatz, originally formulated in the case of the photon structure function, relates to the solution of DGLAP equations formulated in terms of moments. The running time of the implementation is truly modest, even for a large number of iterations, and allows to get a very good accuracy. We hope to return with a discussion of the supersymmetric extension of the method and other applications in the near future.

# Acknowledgments

We thank the Phys. Dept. at the Univ. of Crete and especially Theodore Tomaras for hospitality and partial support under grant HPRN-CT-2000-00131 during this investigation and Marco Stratmann for correspondence. This work is partially supported by INFN (iniz. spec. BA21).

# A Unpolarized kernels

The reference for the unpolarized kernels is [2], rearranged for our purposes. We remind that the plus distribution is defined by

$$\int_0^1 \mathrm{d}x \frac{f(x)}{(1-x)_+} = \int_0^1 \mathrm{d}x \frac{f(x) - f(1)}{1-x} \tag{48}$$

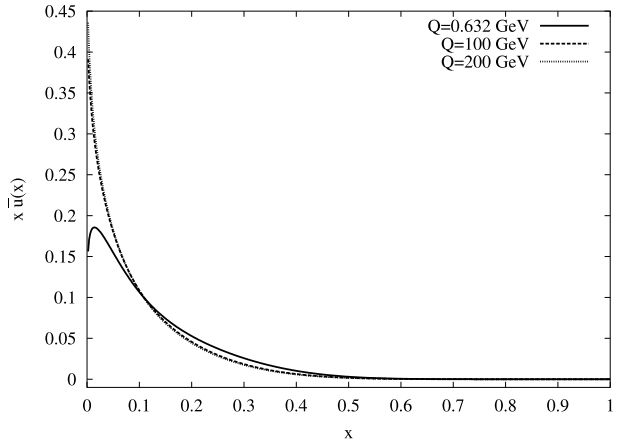


Figure 4: Evolution of the unpolarized antiquark up distribution $x\overline{u}$ versus $x$ at various $Q$ values.

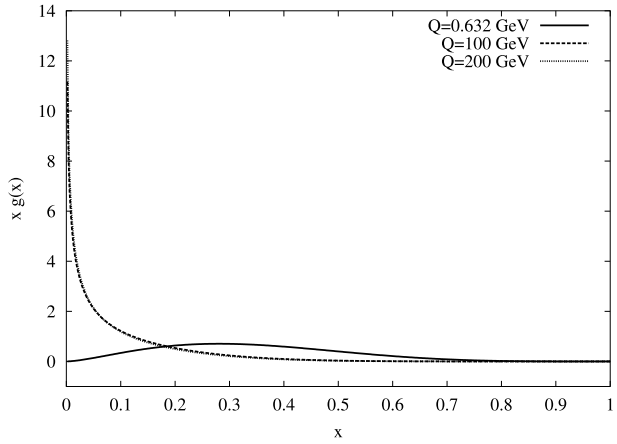


Figure 5: Evolution of the unpolarized gluon distribution $xg$ versus $x$ at various $Q$ values.A

and the Spence function is

$$S_2(x) = -2\mathrm{Li}_2(-x) - 2\log x \log(1+x) + \frac{1}{2}\log^2 x - \frac{\pi^2}{6}, \tag{49}$$

where the dilogarithm is defined by

$$\mathrm{Li}_2(x) = \int_x^0 \frac{\log(1-t)}{t}\mathrm{d}t. \tag{50}$$

$$P_{NS^-}^{(0)}(x) = P_{NS^+}^{(0)}(x) = P_{qq}^{(0)}(x) = C_F\left[\frac{2}{(1-x)_+} - 1 - x + \frac{3}{2}\delta(1-x)\right] \tag{51}$$

$$P_{qg}^{(0)}(x) = 2T_f\left[x^2 + (1-x)^2\right] \tag{52}$$

$$P_{gq}^{(0)}(x) = C_F\left[\frac{1+(1-x)^2}{x}\right] \tag{53}$$

$$P_{gg}^{(0)}(x) = 2N_C\left[\frac{1}{(1-x)_+} + \frac{1}{x} - 2 + x(1-x)\right] + \frac{\beta(0)}{2}\delta(1-x) \tag{54}$$

$$P_{NS^-}^{(1)}(x) \;=\; \left\{\frac{C_F}{18}\left[162C_F(x-1) + 4T_f(11x-1) + N_C(89 - 223x + 3\pi^2(1+x))\right]\right\}$$

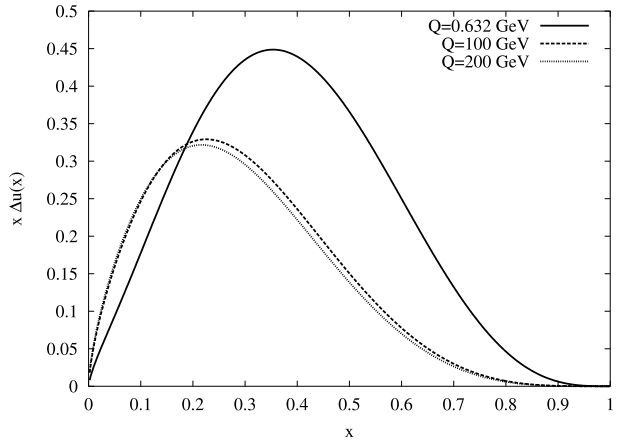


Figure 6: Evolution of the longitudinally polarized quark up distribution $x\Delta u$ versus $x$ at various $Q$ values.

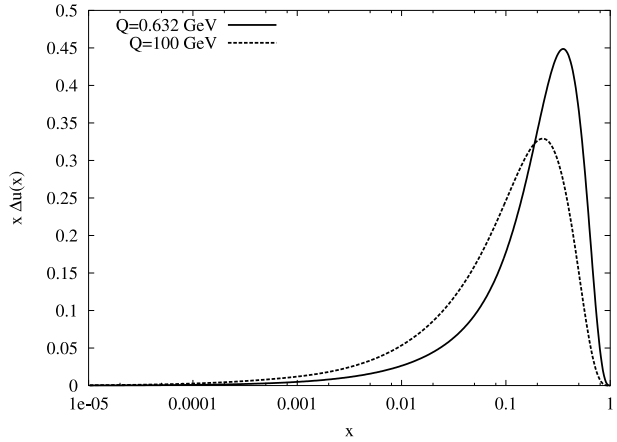


Figure 7: As in figure (6), but now the $x$-axis is in logarithmic scale, to show the small-$x$ behavior.

$$
\begin{aligned}
&+\left\{\frac{C_F\left[30C_F-23N_C+4T_f+12C_Fx+(N_C-24C_F+4T_f)x^2\right]}{6(x-1)}\right\}\log x\\
&+\left\{\frac{C_F\left[C_F-N_C-(C_F+N_C)x^2\right]}{2(x-1)}\right\}\log^2 x\\
&+\left\{\frac{2C_F^2(1+x^2)}{x-1}\right\}\log x\log(1-x)\\
&-\left\{\frac{C_F(2C_F-N_C)(1+x^2)}{1+x}\right\}S_2(x)\\
&-\left\{\frac{C_F}{9}\left[N_C(3\pi^2-67)+20T_f\right]\right\}\frac{1}{(1-x)_+}\\
&+\left\{\frac{C_F}{72}\left[N_C(51+44\pi^2-216\zeta(3))-4T_f(3+4\pi^2)\right.\right.\\
&\qquad\left.\left.+9C_F(3-4\pi^2+48\zeta(3))\right]\right\}\delta(1-x)
\end{aligned}
\tag{55}
$$

$$
\begin{aligned}
P^{(1)}_{NS^+}(x) &= \left\{\frac{C_F}{18}\left[18C_F(x-1)+4T_f(11x-1)+N_C(17-151x+3\pi^2(1+x))\right]\right\}\\
&+\left\{\frac{C_F\left[6C_F(1+2x)-(11N_C-4T_f)(1+x^2)\right]}{6(x-1)}\right\}\log x
\end{aligned}
$$

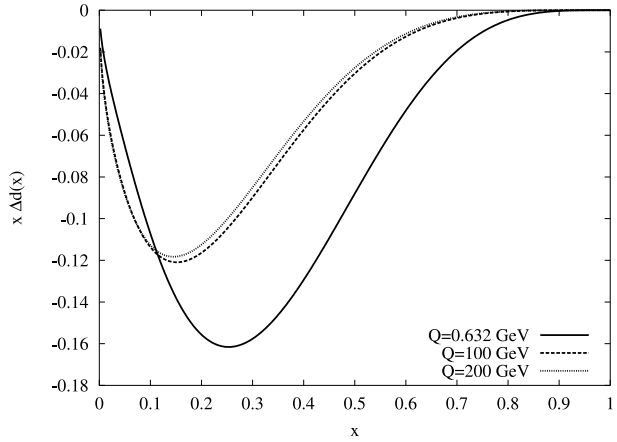


Figure 8: Evolution of $x\Delta d$ versus $x$ at various $Q$ values.

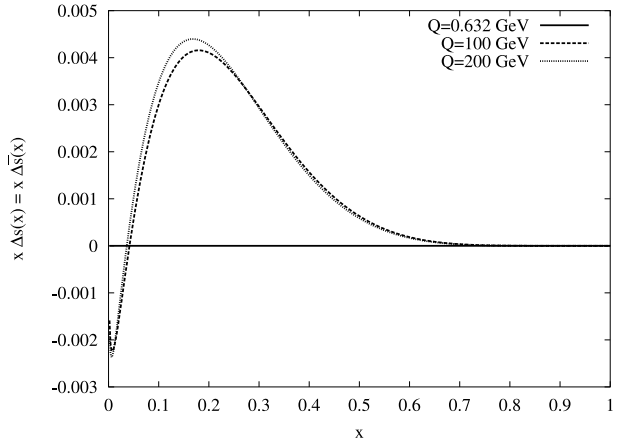


Figure 9: Evolution of $x\Delta s = x\Delta\overline{s}$ versus $x$ at various $Q$ values.

$$
\begin{aligned}
&+\left\{\frac{C_F\left[C_F-N_C-(C_F+N_C)x^2\right]}{2(x-1)}\right\}\log^2 x\\
&+\left\{\frac{2C_F^2(1+x^2)}{x-1}\right\}\log x\log(1-x)\\
&+\left\{\frac{C_F(2C_F-N_C)(1+x^2)}{1+x}\right\}S_2(x)\\
&-\left\{\frac{C_F}{9}\left[N_C(3\pi^2-67)+20T_f\right]\right\}\frac{1}{(1-x)_+}\\
&+\left\{\frac{C_F}{72}\left[N_C(51+44\pi^2-216\zeta(3))-4T_f(3+4\pi^2)\right.\right.\\
&\qquad\left.\left.+9C_F(3-4\pi^2+48\zeta(3))\right]\right\}\delta(1-x)
\end{aligned}
\tag{56}
$$

$$
\begin{aligned}
P_{qq}^{(1)}(x) \;=\;& \frac{C_F}{18x}\left\{x\left[18C_F(x-1)+N_C\left(17-151x+3\pi^2(1+x)\right)\right]\right.\\
&\left.+4T_f\left[20-x\left(19+x(56x-65)\right)\right]\right\}\\
&+\left\{\frac{C_F\left[6C_F(1+2x)-11N_C(1+x^2)+8T_f\left(2x(2x(1+x)-3)-1\right)\right]}{6(x-1)}\right\}\log x\\
&+\left\{\frac{C_F\left[C_F-N_C+4T_f-(C_F+N_C+4T_f)x^2\right]}{2(x-1)}\right\}\log^2 x\\
&+\left\{\frac{2C_F^2(1+x^2)}{x-1}\right\}\log x\log(1-x)
\end{aligned}
$$

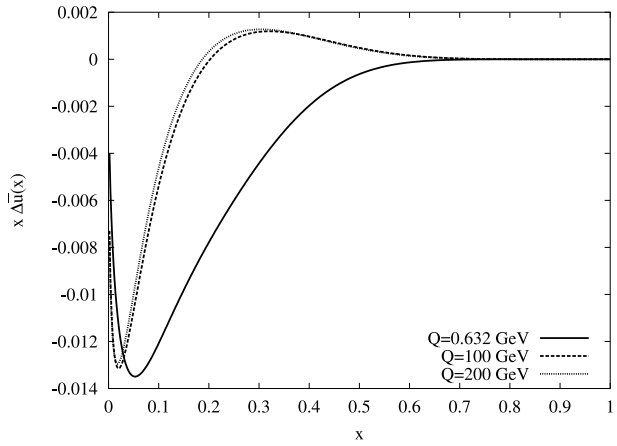


Figure 10: Evolution of the longitudinally polarized antiquark up distribution $x\Delta\overline{u}$ versus $x$ at various $Q$ values.

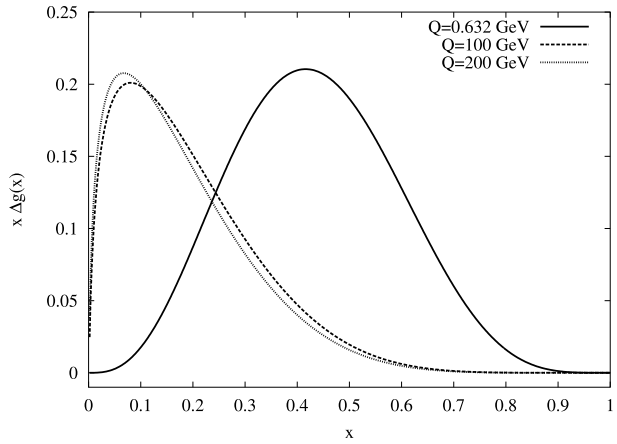


Figure 11: Evolution of the longitudinally polarized gluon distribution $x\Delta g$ versus $x$ at various $Q$ values.

$$
\begin{aligned}
&+\left\{\frac{C_F(2C_F-N_C)(1+x^2)}{1+x}\right\}S_2(x)\\
&-\left\{\frac{C_F}{9}\left[N_C(3\pi^2-67)+20T_f\right]\right\}\frac{1}{(1-x)_+}\\
&+\left\{\frac{C_F}{72}\left[N_C(51+44\pi^2-216\zeta(3))-4T_f(3+4\pi^2)\right.\right.\\
&\qquad\left.\left.+9C_F(3-4\pi^2+48\zeta(3))\right]\right\}\delta(1-x) \qquad (57)
\end{aligned}
$$

$$
\begin{aligned}
P_{qg}^{(1)}(x) \;=\;& \left\{\frac{1}{9x}\left[T_f\left(3C_Fx(42-87x+60x^2-\pi^2(2+4(x-1)x))\right.\right.\right.\\
&\left.\left.\left.+N_C(40+x(450x-36-436x^2+\pi^2(3+6(x-1)x)))\right)\right]\right\}\\
&+\left\{\frac{T_f}{3}\left[6N_C+8N_Cx(6+11x)+3C_F(3-4x+8x^2)\right]\right\}\log x\\
&+\left\{8(C_F-N_C)T_f(1-x)x\right\}\log(1-x)\\
&+\left\{T_f\left[C_F(1-2x+4x^2)-N_C(3+2x(3+x))\right]\right\}\log^2 x\\
&+\left\{2(C_F-N_C)T_f\left[1+2(x-1)x\right]\right\}\log^2(1-x)\\
&-\left\{4C_FT_f\left[1+2(x-1)x\right]\right\}\log x\log(1-x)\\
&+\left\{2N_CT_f\left[1+2x(1+x)\right]\right\}S_2(x) \qquad (58)
\end{aligned}
$$

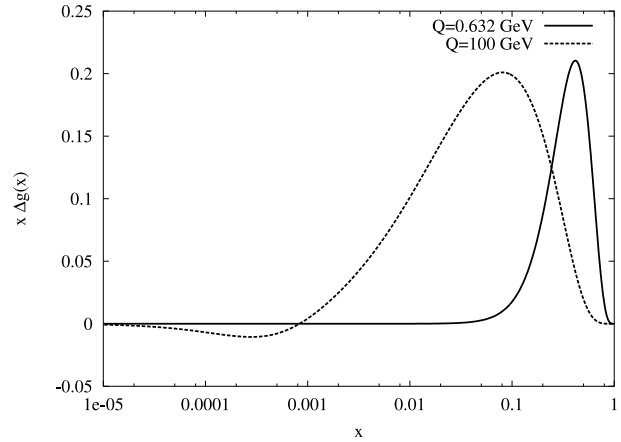


Figure 12: As in figure (11), but now the $x$-axis is in logarithmic scale.

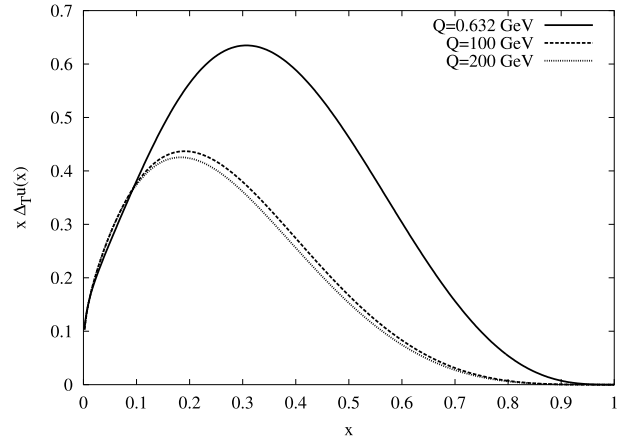


Figure 13: Evolution of the transversely polarized quark up distribution $x\Delta_T u$ versus $x$ at various $Q$ values.

$$
\begin{aligned}
P_{gq}^{(1)}(x) &= \left\{\frac{1}{18x}\left[C_F\left(N_C(18-3\pi^2(2+(x-2)x)+2x(19+x(37+44x)))\right.\right.\right. \\
&\qquad \left.\left.\left. -9C_F x(5+7x)-16T_f(5+x(4x-5)))\right]\right\} \\
&+\left\{\frac{C_F}{6}\left[3C_F(4+7x)-2N_C\left(36+x(15+8x)\right)\right]\right\}\log x \\
&+\left\{\frac{C_F}{3x}\left[N_C\left(22+x(17x-22)\right)-4T_f\left(2+(x-2)x\right)\right.\right. \\
&\qquad \left.\left. -3C_F\left(6+x(5x-6)\right)\right]\right\}\log(1-x) \\
&+\left\{\frac{C_F}{2x}\left[C_F(x-2)x+N_C\left(2+3x(2+x)\right)\right]\right\}\log^2 x \\
&+\left\{\frac{C_F(N_C-C_F)\left[2+(x-2)x\right]}{x}\right\}\log^2(1-x) \\
&-\left\{\frac{2C_F N_C\left(2+(x-2)x\right)}{x}\right\}\log x\log(1-x) \\
&-\left\{\frac{C_F N_C\left(2+x(2+x)\right)}{x}\right\}S_2(x) \qquad (59)
\end{aligned}
$$

$$
\begin{aligned}
P_{gg}^{(1)}(x) &= \left\{\frac{1}{18x}\left[24C_F T_f(x-1)\left(x(11+5x)-1\right)+4N_C T_f\left(x(29+x(23x-19))-23\right)\right.\right. \\
&\qquad \left.\left. +N_C^2\left(6\pi^2(x(2+(x-1)x)-1)-x(25+109x)\right)\right]\right\}
\end{aligned}
$$

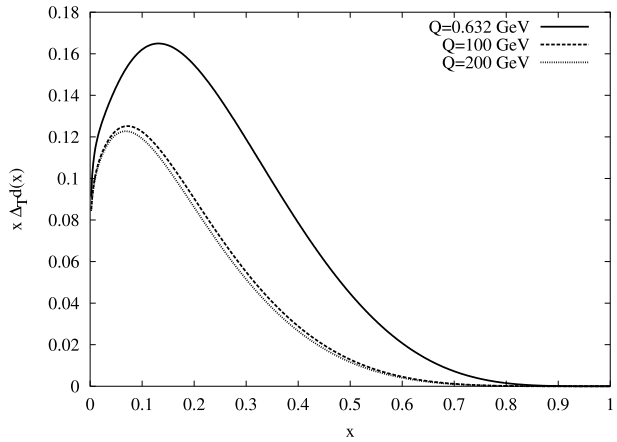


Figure 14: Evolution of $x\Delta_T d$ versus $x$ at various $Q$ values.

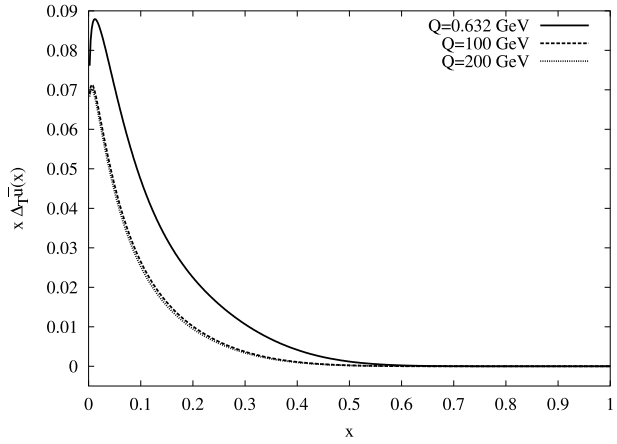


Figure 15: Evolution of the transversely polarized antiquark up distribution $x\Delta_T\overline{u}$ versus $x$ at various $Q$ values.

$$
\begin{aligned}
&+\left\{\frac{N_C^2\left[11(1-4x)x-25\right]-4N_CT_f(1+x)-6C_FT_f(3+5x)}{3}\right\}\log x\\
&+\left\{\frac{2C_FT_fx(x^2-1)+N_C^2\left[1+x\left(2+x(3+(x-6)x)\right)\right]}{(1-x)x}\right\}\log^2 x\\
&+\left\{\frac{4N_C^2\left[1+(x-1)x\right]^2}{(x-1)x}\right\}\log x\log(1-x)\\
&-\left\{\frac{2N_C^2\left(1+x+x^2\right)^2}{x(1+x)}\right\}S_2(x)\\
&-\left\{\frac{N_C}{9}\left[N_C(3\pi^2-67)+20T_f\right]\right\}\frac{1}{(1-x)_+}\\
&+\left\{\frac{N_C}{3}\left[N_C(8+9\zeta(3))-4T_f\right]-C_FT_f\right\}\delta(1-x)
\end{aligned}
\tag{60}
$$

# B Longitudinally polarized kernels

The reference for the longitudinally polarized kernels is [11].

$$
\Delta P_{NS^-}^{(0)}(x)=\Delta P_{NS^+}^{(0)}(x)=\Delta P_{qq}^{(0)}(x)=C_F\left[\frac{2}{(1-x)_+}-1-x+\frac{3}{2}\delta(1-x)\right] \tag{61}
$$

$$\Delta P_{qg}^{(0)}(x) = 2T_f(2x-1) \tag{62}$$

$$\Delta P_{gq}^{(0)}(x) = C_F(2-x) \tag{63}$$

$$\Delta P_{gg}^{(0)}(x) = 2N_C\left[\frac{1}{(1-x)_+} - 2x + 1\right] + \frac{\beta(0)}{2}\delta(1-x) \tag{64}$$

$$\Delta P_{NS^-}^{(1)}(x) = P_{NS^+}^{(1)}(x) \tag{65}$$

$$\Delta P_{NS^+}^{(1)}(x) = P_{NS^-}^{(1)}(x) \tag{66}$$

$$\begin{aligned}
\Delta P_{qq}^{(1)}(x) &= \left\{\frac{C_F}{18}\left[162C_F(x-1) + 8T_f(4+z) + N_C\left(89 - 223x + 3\pi^2(1+x)\right)\right]\right\} \\
&+ \left\{\frac{C_F}{6(x-1)}\left[N_C(x^2-23) - 6C_F(4x^2-2x-5)\right.\right. \\
&\qquad \left.\left. +8T_f\left(2 + x(5x-6)\right)\right]\right\}\log x \\
&+ \left\{\frac{C_F\left[C_F - N_C + 4T_f - (C_F + N_C + 4T_f)x^2\right]}{2(x-1)}\right\}\log^2 x \\
&+ \left\{\frac{2C_F^2(1+x^2)}{x-1}\right\}\log x\log(1-x) \\
&- \left\{\frac{C_F(2C_F - N_C)(1+x^2)}{1+x}\right\}S_2(x) \\
&- \left\{\frac{C_F}{9}\left[N_C(3\pi^2 - 67) + 20T_f\right]\right\}\frac{1}{(1-x)_+} \\
&+ \left\{\frac{C_F}{72}\left[N_C(51 + 44\pi^2 - 216\zeta(3)) - 4T_f(3 + 4\pi^2)\right.\right. \\
&\qquad \left.\left. +9C_F(3 - 4\pi^2 + 48\zeta(3))\right]\right\}\delta(1-x)
\end{aligned} \tag{67}$$

$$\begin{aligned}
\Delta P_{qg}^{(1)}(x) &= \left\{\frac{T_f}{3}\left[C_F\left(\pi^2(2-4x) - 66 + 81x\right) + N_C\left(72 - 66x + \pi^2(2x-1)\right)\right]\right\} \\
&+ \left\{T_f\left[2N_C(1+8x) - 9C_F\right]\right\}\log x \\
&+ \left\{8(N_C - C_F)T_f(x-1)\right\}\log(1-x) \\
&+ \left\{T_f\left[C_F(2x-1) - 3N_C(1+2x)\right]\right\}\log^2 x \\
&+ \left\{2(C_F - N_C)T_f(2x-1)\right\}\log^2(1-x) \\
&+ \left\{4C_FT_f(1-2x)\right\}\log x\log(1-x) \\
&+ \left\{2N_CT_f(1+2x)\right\}S_2(x)
\end{aligned} \tag{68}$$

$$\begin{aligned}
\Delta P_{gq}^{(1)}(x) &= \left\{\frac{C_F}{18}\left[9C_F(8x-17) - 8T_f(4+x) + N_C\left(82 + 3\pi^2(x-2) + 70x\right)\right]\right\} \\
&+ \left\{\frac{C_F}{2}\left[N_C(8-26x) + C_F(x-4)\right]\right\}\log x \\
&+ \left\{\frac{C_F}{3}\left[4T_f(x-2) - 3C_F(2+x) + N_C(10+x)\right]\right\}\log(1-x) \\
&+ \left\{\frac{C_F}{2}\left[3N_C(2+x) - C_F(x-2)\right]\right\}\log^2 x \\
&+ \left\{C_F(C_F - N_C)(x-2)\right\}\log^2(1-x) \\
&+ \left\{2C_FN_C(x-2)\right\}\log x\log(1-x) \\
&- \left\{C_FN_C(2+x)\right\}S_2(x)
\end{aligned} \tag{69}$$

$$
\begin{aligned}
\Delta P_{gg}^{(1)}(x) &= \left\{\frac{1}{18}\left[180C_FT_f(x-1)+8N_CT_f(19x-4)+N_C^2\left(6\pi^2(1+2x)-305-97x\right)\right]\right\} \\
&+\left\{\frac{1}{3}\left[N_C^2(29-67x)+6C_FT_f(x-5)-4N_CT_f(1+x)\right]\right\}\log x \\
&+\left\{\frac{N_C^2(2x^2+x-4)-2C_FT_f(x^2-1)}{x-1}\right\}\log^2 x \\
&+\left\{\frac{4N_C^2x(2x-1)}{x-1}\right\}\log x\log(1-x) \\
&-\left\{\frac{2N_C^2x(1+2x)}{1+x}\right\}S_2(x) \\
&-\left\{\frac{N_C}{9}\left[N_C(3\pi^2-67)+20T_f\right]\right\}\frac{1}{(1-x)_+} \\
&+\left\{\frac{1}{3}\left[N_C^2(8+9\zeta(3))-3C_FT_f-4N_CT_f\right]\right\}\delta(1-x) \qquad (70)
\end{aligned}
$$

# C Kernels in the helicity basis

The expression of the kernels in the helicity basis given below are obtained combining the NLO computations of [2, 11]

$$
\begin{aligned}
P_{NS^-,++}^{(1)}(x) &= \left\{\frac{C_F}{18}\left[90C_F(x-1)+4T_f(11x-1)+N_C(53-187x+3\pi^2(1+x))\right]\right\} \\
&+\left\{\frac{C_F\left[6C_F(3-2(x-1)x)+4T_f(1+x^2)-N_C(17+5x^2)\right]}{6(x-1)}\right\}\log x \\
&+\left\{\frac{C_F\left[C_F-N_C-(C_F+N_C)x^2\right]}{2(x-1)}\right\}\log^2 x \\
&+\left\{\frac{2C_F^2(1+x^2)}{x-1}\right\}\log x\log(1-x) \\
&+\left\{-\frac{C_F}{9}\left[N_C(3\pi^2-67)+20T_f\right]\right\}\frac{1}{(1-x)_+} \\
&+\left\{C_F\left[\frac{N_C(51+44\pi^2)-4T_f(3+4\pi^2)}{72}-3N_C\zeta(3)\right.\right. \\
&\qquad \left.\left.+C_F\left(\frac{3}{8}-\frac{\pi^2}{2}+6\zeta(3)\right)\right]\right\}\delta(1-x) \qquad (71)
\end{aligned}
$$

$$
\begin{aligned}
P_{NS^-,+-}^{(1)}(x) &= \{2C_F(2C_F-N_C)(x-1)\} \\
&+\{C_F(N_C-2C_F)(1+x)\}\log x \\
&+\left\{\frac{C_F(N_C-2C_F)(1+x^2)}{1+x}\right\}S_2(x) \qquad (72)
\end{aligned}
$$

$$
P_{NS^+,++}^{(1)}(x) = P_{NS^-,++}^{(1)}(x) \qquad (73)
$$

$$
P_{NS^+,+-}^{(1)}(x) = -P_{NS^-,+-}^{(1)}(x) \qquad (74)
$$

$$
P_{qq,++}^{(1)}(x) = \left\{\frac{C_F}{18x}\left[2T_f(20-(x-1)x(56x-11))\right.\right.
$$

$$
\begin{aligned}
&\qquad +x(90C_F(x-1)+N_C(53-187x+3\pi^2(1+x)))\Big]\Big\}\\
&+\left\{\frac{C_F}{6(x-1)}\Big[6C_F(3-2(x-1)x)-N_C(17+5x^2)\right.\\
&\qquad \left.+4T_f(1+x(x(9+4x)-12))\Big]\right\}\log x\\
&+\left\{\frac{C_F\left[C_F-N_C+4T_f-(C_F+N_C+4T_F)x^2\right]}{2(x-1)}\right\}\log^2 x\\
&+\left\{\frac{2C_F^2(1+x^2)}{x-1}\right\}\log x\log(1-x)\\
&+\left\{-\frac{C_F}{9}\Big[N_C(3\pi^2-67)+20T_f\Big]\right\}\frac{1}{(1-x)_+}\\
&+\left\{\frac{C_F}{72}\Big[N_C(51+44\pi^2-216\zeta(3))-4T_f(3+4\pi^2)\right.\\
&\qquad \left.+9C_F(3-4\pi^2+48\zeta(3))\Big]\right\}\delta(1-x) \qquad (75)
\end{aligned}
$$

$$
\begin{aligned}
P^{(1)}_{qq,+-}(x) &= \left\{\frac{C_F(1-x)}{9x}\Big[18(2C_F-N_C)x+T_f(20-7x+56x^2)\Big]\right\}\\
&+\left\{\frac{C_F}{3}\left[6C_F(1+x)-3N_C(1+x)+2T_f(3+x(3+4x))\right]\right\}\log x\\
&+\left\{\frac{C_F(2C_F-N_C)(1+x^2)}{1+x}\right\}S_2(x) \qquad (76)
\end{aligned}
$$

$$
\begin{aligned}
P^{(1)}_{qg,++}(x) &= \Big\{\frac{T_f}{9x}\Big[N_C(20+x(90+x(126+(3\pi^2-218)x)))\\
&\qquad -3C_Fx(12-x(2(15-\pi^2)x-3))\Big]\Big\}\\
&+\left\{\frac{T_f}{3}\Big[6N_C+4N_Cx(12+11x)-3C_F(3+2x-4x^2)\Big]\right\}\log x\\
&+\Big\{4T_f(C_F-N_C)(1-x^2)\Big\}\log(1-x)\\
&+\Big\{T_f\Big[2C_Fx^2-N_C(3+x(6+x))\Big]\Big\}\log^2 x\\
&+\Big\{2T_f(C_F-N_C)x^2\Big\}\log^2(1-x)\\
&+\Big\{-4C_FT_fx^2\Big\}\log x\log(1-x)\\
&+\Big\{2N_CT_f(1+x)^2\Big\}S_2(x) \qquad (77)
\end{aligned}
$$

$$
\begin{aligned}
P^{(1)}_{qg,+-}(x) &= \left\{\frac{T_f(x-1)}{9x}\Big[6C_Fx(15x-27-\pi^2(x-1))\right.\\
&\qquad \left.-N_C(20-(106+3\pi^2(x-1)-218x)x)\Big]\right\}\\
&+\left\{\frac{2}{3}T_f\Big[22N_Cx^2+3C_F(3+x(2x-1))\Big]\right\}\log x\\
&+\Big\{4T_f(N_C-C_F)(1-x)^2\Big\}\log(1-x)\\
&+\Big\{T_f\Big[C_F(1+2(x-1)x)-N_Cx^2\Big]\Big\}\log^2 x\\
&+\Big\{2T_f(C_F-N_C)(1-x)^2\Big\}\log^2(1-x)\\
&+\Big\{-4C_FT_f(1-x)^2\Big\}\log x\log(1-x)\\
&+\Big\{2N_CT_fx^2\Big\}S_2(x) \qquad (78)
\end{aligned}
$$

$$
\begin{aligned}
P^{(1)}_{gq,++}(x) &= \left\{\frac{C_F}{36x}\left[9C_F(x-22)x - 8T_f(10+3x(3x-2))\right.\right. \\
&\qquad \left.\left. +2N_C(9-3\pi^2+4x(15+x(18+11x)))\right]\right\} \\
&+\left\{\frac{C_F}{3}\left[6C_Fx - N_C(12+x(27+4x))\right]\right\}\log x \\
&+\left\{\frac{C_F}{3x}\left[N_C(11-3(2-3x)x) - 4T_f - 3C_F(3+x(3x-2))\right]\right\}\log(1-x) \\
&+\left\{\frac{C_FN_C(1+3x(2+x))}{2x}\right\}\log^2 x \\
&+\left\{\frac{C_F(N_C-C_F)}{x}\right\}\log^2(1-x) \\
&+\left\{-\frac{2C_FN_C}{x}\right\}\log x\log(1-x) \\
&+\left\{-\frac{C_FN_C(1+x)^2}{x}\right\}S_2(x) \qquad (79)
\end{aligned}
$$

$$
\begin{aligned}
P^{(1)}_{gq,+-}(x) &= \left\{\frac{C_F}{36x}\left[27C_F(4-5x)x - 8T_f(10+7(x-2)x)\right.\right. \\
&\qquad \left.\left. +2N_C(9-3\pi^2(x-1)^2 - 2x(11-x-22x^2))\right]\right\} \\
&+\left\{\frac{C_F}{6}\left[3C_F(4+3x) - 8N_C(6+(x-3)x)\right]\right\}\log x \\
&+\left\{\frac{C_F}{3x}\left[N_C(11+8(x-2)x) - 4T_f(1-x)^2\right.\right. \\
&\qquad \left.\left. -3C_F(3+2(x-2)x)\right]\right\}\log(1-x) \\
&+\left\{\frac{C_F}{2x}\left[N_C + C_F(x-2)x\right]\right\}\log^2 x \\
&+\left\{-\frac{C_F(C_F-N_C)(x-1)^2}{x}\right\}\log^2(1-x) \\
&+\left\{-\frac{2C_FN_C(x-1)^2}{x}\right\}\log x\log(1-x) \\
&+\left\{-\frac{C_FN_c}{x}\right\}S_2(x) \qquad (80)
\end{aligned}
$$

$$
\begin{aligned}
P^{(1)}_{gg,++}(x) &= \left\{\frac{1}{18x}\left[6C_FT_f(x-1)(x(37+10x)-2)\right.\right. \\
&\qquad +2C_FT_f(x(21+x(19+23x))-23) \\
&\qquad \left.\left. +N_C^2(3\pi^2(x(3+x+x^2)-1) - x(165+103x))\right]\right\} \\
&+\left\{-\frac{2}{3}\left[2N_CT_f(1+x) + 6C_FT_f(2+x) + N_C^2(x(14+11x)-1)\right]\right\}\log x \\
&+\left\{\frac{4C_FT_fx(x^2-1) + N_C^2(1+x(6+x(2+(x-8)x)))}{2(1-x)x}\right\}\log^2 x \\
&+\left\{\frac{2N_C^2(1-x(2-2x-x^3))}{(x-1)x}\right\}\log x\log(1-x) \\
&+\left\{-\frac{N_C^2(1+x+3x^2+x^3)}{x}\right\}S_2(x)
\end{aligned}
$$

$$+\left\{\frac{N_C}{9}\left[N_C(67-3\pi^2)-20T_f\right]\right\}\frac{1}{(1-x)_+}$$
$$+\left\{N_C^2\left(\frac{8}{3}+3\zeta(3)\right)-C_FT_f-\frac{4N_CT_f}{3}\right\}\delta(1-x) \tag{81}$$

$$\begin{aligned}
P^{(1)}_{gg,+-}(x) &= \left\{\frac{1}{18x}\left[6C_FT_f(x-1)(x(7+10x)-2)\right.\right.\\
&\qquad +N_C^2(2(70-3x)x-3\pi^2(1-x+3x^2-x^3))\\
&\qquad \left.\left.+2N_CT_f(x(37+x(23x-57))-23)\right]\right\}\\
&+\left\{2C_FT_f(1-3x)-N_C^2\left(9-13x+\frac{22x^2}{3}\right)\right\}\log x\\
&+\left\{\frac{N_c^2}{2x}\left(1-x+3x^2-x^3\right)\right\}\log^2 x\\
&+\left\{\frac{2N_C^2}{x}\left(x^3-3x^2+x-1\right)\right\}\log x\log(1-x)\\
&+\left\{-\frac{N_C^2(1+x(2+2x+x^3))}{x(1+x)}\right\}S_2(x)
\end{aligned} \tag{82}$$

# D Transversely polarized kernels

The reference for the transversely polarized kernels is [12].

$$\Delta_TP^{(0)}_{NS^-}(x)=\Delta_TP^{(0)}_{NS^+}(x)=C_F\left[\frac{2}{(1-x)_+}-2+\frac{3}{2}\delta(1-x)\right] \tag{83}$$

$$\begin{aligned}
\Delta_TP^{(1)}_{NS^-} &= \left\{\frac{C_F}{9}\left[20T_f-18C_F(x-1)+N_C(9x-76+3\pi^2)\right]\right\}\\
&+\left\{\frac{C_F(9C_F-11N_C+4T_f)x}{3(x-1)}\right\}\log x\\
&+\left\{\frac{C_FN_Cx}{1-x}\right\}\log^2 x\\
&+\left\{\frac{4C_F^2x}{x-1}\right\}\log x\log(1-x)\\
&+\left\{\frac{2C_F(2C_F-N_C)x}{1+x}\right\}S_2(x)\\
&-\left\{\frac{C_F}{9}\left[N_C(3\pi^2-67)+20T_f\right]\right\}\frac{1}{(1-x)_+}\\
&+\left\{\frac{C_F}{72}\left[N_C(51+44\pi^2-216\zeta(3))-4T_f(3+4\pi^2)\right.\right.\\
&\qquad \left.\left.+9C_F(3-4\pi^2+48\zeta(3))\right]\right\}\delta(1-x)
\end{aligned} \tag{84}$$

$$\begin{aligned}
\Delta_TP^{(1)}_{NS^+} &= \left\{\frac{C_F}{9}\left[N_C(3\pi^2-67)+20T_f\right]\right\}\\
&+\left\{\frac{C_F(9C_F-11N_C+4T_f)x}{3(x-1)}\right\}\log x
\end{aligned}$$

$$
\begin{aligned}
&+\left\{\frac{C_F N_C x}{1-x}\right\}\log^2 x \\
&+\left\{\frac{4C_F^2 x}{x-1}\right\}\log x\log(1-x) \\
&+\left\{\frac{2C_F(N_C-2C_F)x}{1+x}\right\}S_2(x) \\
&-\left\{\frac{C_F}{9}\left[N_C(3\pi^2-67)+20T_f\right]\right\}\frac{1}{(1-x)_+} \\
&+\left\{\frac{C_F}{72}\left[N_C(51+44\pi^2-216\zeta(3))-4T_f(3+4\pi^2)\right.\right. \\
&\qquad\left.\left.+9C_F(3-4\pi^2+48\zeta(3))\right]\right\}\delta(1-x) \qquad (85)
\end{aligned}
$$

# References


[1] M. Hirai, S. Kumano and Myiama, Comput. Phys. Commun.**108** (1998), 38; R. Kobayashi, M. Konuma and S. Kumano, Comput. Phys. Commun.**86** (1995), 264.

[2] W. Furmanski and R. Petronzio, Nucl. Phys. **B 195** (1982) 237.

[3] C. Corianò and C. Savkli, Comput.Phys.Commun.**118**(1999) 236.

[4] G.Rossi, Phys.Rev.D **29** (1984) 852.

[5] J.H. Da Luz Vieira and J. K. Storrow, Z.Phys. **C51** (1991) 241.

[6] L.E. Gordon and G. P. Ramsey, Phys. Rev. **D59** (1999), 074018.

[7] M.Glück, E.Reya and A.Vogt, Eur.Phys.J.C **5** (1998) 461

[8] M.Glück, E.Reya, M.Stratmann and W.Vogelsang, Phys.Rev.D **63** (2001) 094005.

[9] O.Martin, A.Schäfer, M.Stratmann and W.Vogelsang, Phys.Rev.D **57** (1998) 3084.

[10] W.H.Press, S.A.Teukolsky, W.T.Vetterling and B.P.Flannery, *Numerical recipes in C*, Cambridge University Press (1992).

[11] W.Vogelsang, Nucl.Phys.B **475** (1996) 47

[12] W.Vogelsang, Phys.Rev.D **57** (1998) 1886

[13] A. Cafarella, C.Corianò and M.Guzzi, hep-ph/0303050

[14] L.E.Gordon, M.Goshtasbpour and G.P.Ramsey, Phys.Rev.D **58** (1998) 094017

[15] H.L.Lai et al., Phys.Rev.D **55** (1997) 1280